Received: 23 October 2019 | Revised: 5 March 2020 | Accepted: 29 March 2020

DOI: 10.1111/cmi.13207

RESEARCH ARTICLE

WILEY

Transmigration of *Trypanosoma cruzi* trypomastigotes through 3D cultures resembling a physiological environment

Matías Exequiel Rodríguez[1] | Mariana Rizzi[1] | Lucas D. Caeiro[1] | Yamil E. Masip[1] | Alina Perrone[2] | Daniel O. Sánchez[1] | Jacqueline Búa[2] | Valeria Tekiel[1]

[1]Instituto de Investigaciones Biotecnológicas "Dr. R. Ugalde" (IIBIO) Universidad Nacional de San Martín (UNSAM)—CONICET, Buenos Aires, Argentina

[2]Instituto Nacional de Parasitología "Dr Mario Fatala Chaben", ANLIS-Carlos G. Malbrán, Buenos Aires, Argentina

Correspondence
Valeria Tekiel, Instituto de Investigaciones Biotecnológicas "Dr. Rodolfo A. Ugalde" (IIBIO), Universidad Nacional de San Martín, UNSAM-CONICET, Av. 25 de Mayo y Francia, San Martín (B1650KNA), Buenos Aires, Argentina.
Email: valet@iib.unsam.edu.ar or
Email: vtekiel@gmail.com.

Funding information
ANPCyT/FONCyT, Grant/Award Numbers: PICT 2017-2644, PICT-2016-0108

Abstract

To disseminate and colonise tissues in the mammalian host, *Trypanosoma cruzi* trypomastogotes should cross several biological barriers. How this process occurs or its impact in the outcome of the disease is largely speculative. We examined the *in vitro* transmigration of trypomastigotes through three-dimensional cultures (spheroids) to understand the tissular dissemination of different *T. cruzi* strains. Virulent strains were highly invasive: trypomastigotes deeply transmigrate up to 50 μm inside spheroids and were evenly distributed at the spheroid surface. Parasites inside spheroids were systematically observed in the space between cells suggesting a paracellular route of transmigration. On the contrary, poorly virulent strains presented a weak migratory capacity and remained in the external layers of spheroids with a patch-like distribution pattern. The invasiveness—understood as the ability to transmigrate deep into spheroids—was not a transferable feature between strains, neither by soluble or secreted factors nor by co-cultivation of trypomastigotes from invasive and non-invasive strains. Besides, we demonstrated that *T. cruzi* isolates from children that were born congenitally infected presented a highly migrant phenotype while an isolate from an infected mother (that never transmitted the infection to any of her children) presented significantly less migration. In brief, we demonstrated that in a 3D microenvironment each strain presents a characteristic migration pattern that can be associated to their *in vivo* behaviour. Altogether, data presented here repositionate spheroids as a valuable tool to study host–pathogen interactions.

KEYWORDS

3D cultures, Chagas disease, congenital infection, spheroids, transmigration, *Trypanosoma cruzi*, trypomastigotes

1 | INTRODUCTION

The protozoan parasite *Trypanosoma cruzi* is the etiological agent of Chagas disease, which currently affects about 8 million people. Chagas' disease is an endemic illness in Latin America that has spread worldwide in the past years. The infection usually develops as a chronic cardiac, digestive or neurologic pathology. The reason why symptoms appear 10 or more years after the initial infection, and only in ~40% of individuals, remains unsolved, but both host and parasite genetic background should have an impact on the disease outcome. Chagas disease is one of the main health problems in Latin America, causing more than 10,000 deaths per year, and incapacity in infected individuals (OPS OMS, 2015).

In humans, the infection initiates with trypomastigotes deposited on mucous or skin, along with triatomine bug faeces, when the insect

vector feeds on blood. Trypomastigotes are able to invade any nucleate cells at the infection site. Once inside the cell, trypomastigotes differentiate to amastigotes, which are the intracellular and replicative form. After several division cycles, amastigotes differentiate again into trypomastigotes, the infected cells burst, and parasites are released into the interstitial space. Trypomastigotes can either infect neighbouring cells or spread distantly by circulation. Successive cycles of intracellular infection and replication followed by bloodstream trypomastigote dissemination are the hallmark of the initial acute phase, which drives the amplification of the parasitic load, and eventually produces the infection of organs and tissues (Andrade & Andrews, 2005). The acute phase ends approximately 2–3 months after the initial infection, the time required by the host immune system to control parasitemia and clear most trypomastigotes from peripheral circulation. However, a chronic and persistent infection is already established, characterised by the presence of intracellular amastigotes essentially confined into tissues along with positive serologic tests (Andrade & Andrews, 2005; Rassi, Rassi, & Marin-Neto, 2010).

The experimental murine model allowed to understand that during the acute phase, trypomastigotes disseminate from the inoculation site to almost all tissues, to render completely parasitized mice, few days after the initial infection (Lewis, Francisco, Taylor, Jayawardhana, & Kelly, 2016). This entails that trypomastigotes should be able to escape from peripheral circulation, cross the vascular endothelium and migrate through the extracellular matrix (ECM) to establish a tissular intracellular infection (Costa et al., 2018). The effectiveness of trypomastigotes to cross biological barriers and migrate through tissues will impact on *T. cruzi* ability to produce a severe, moderate or mild tissue infection. This process—that can be linked to parasite virulence and dynamic of infection *in vivo*—is poorly understood. Some authors suggested that the rupture of the endothelial barrier is necessary for the infection of target tissues (Prado et al., 2011). On the contrary, others showed that trypomastigotes traverse the endothelial barrier involving a transcellular traffic of trypomastigotes through endothelial cells, mediated by the activation of the bradykinin receptor 2, and without disturbing its integrity nor its permeability (Coates et al., 2013). Since different combinations of parasite and mouse strains present differential tissue colonisation and target organs of damage (Lewis et al., 2014; Santi-Rocca, Gironès, & Fresno, 2019), the differences between both proposed transmigration models could be attributed to the different strains employed. Either way, trypomastigote transmigration through tissues is an essential event for *T. cruzi* infection. Studies on *T. cruzi* transmigration have been very limited, probably because of the extremely simplicity of monolayers cultures and—on the other hand—the complexity of *in vivo* models, which present low spatio-temporal resolution. Three-dimensional (3D) cultures are physiologically relevant and a good alternative because they mimic the microarchitecture of tissues and can provide an environment similar to the encountered in natural infections (Shamir & Ewald, 2014).

Spheroids are small aggregates of cells that do not adhere to a culture substrate and grow in 3D. Cells interact with each other and secrete the ECM in which they reside, resembling their original microenvironment both functionally and structurally (Fennema, Rivron, Rouwkema, van Blitterswijk, & de Boer, 2013; Zanoni et al., 2016). Spheroids have been broadly employed and deeply contribute to understand mechanisms in cancer biology and immunology (Baruzzi et al., 2015; Giannattasio et al., 2015; Rohland et al., 2015), but they have rarely been employed to explore infectious diseases and host–parasite interactions. Remarkably, the co-culture of spheroids of myocytes with *T. cruzi* trypomastigotes has demonstrated to be an accurate model of fibrosis and hypertrophy that adequately recreates the chronic chagasic cardiomyopathy (Ferrão et al., 2018; Garzoni et al., 2008). In the present work we took advantage of the 3D spheroid technology to disclose how trypomastigotes transmigrate across tissues, which is a key process of the host–parasite interplay in the early steps of infection. We demonstrate that the invasiveness of trypomastigotes from different *T. cruzi* strains and isolates into spheroids can be associated with their *in vivo* behaviour and virulence.

2 | RESULTS

2.1 | *T. cruzi* trypomastigotes are less infective in 3D spheroids than in 2D monolayer cultures

T. cruzi presents a high genetic heterogeneity and, currently, *T. cruzi* strains are classified into six clusters or DTUs, named TcI to TcVI (Zingales et al., 2012). We selected CL Brener (DTU TcVI) and SylvioX10 (DTU TcI) strains, of high and low virulence, respectively, and whose biologically distinctive behaviour in experimental models of *T. cruzi* infection is well characterised, (Belew et al., 2017; Lewis et al., 2014; Marinho et al., 2007; Marinho et al., 2009).

HeLa cells constitutively expressing LifeAct-RFP (HelaR2 hereon), along with trypomastigotes labelled with CFSE or CTFR were employed to monitor short-time infection dynamics and host–parasite interactions (Figure 1). We first evaluated the infection profile of trypomastigotes both on conventional 2D monolayers and in 3D spheroids (Figure 2). While on conventional 2D monolayer cultures CL Brener and SylvioX10 parasites showed similar infection rates (~70%) (Figure 2a,c), both strains were much less effective to infect 3D spheroids (Figure 2b,c) and with differences between both strains. Infection with CL Brener rendered higher number of cells with cell-attached or internalised parasites (38.2% CL Brener vs 8.5% SylvioX10), as detected by flow cytometry of disaggregated spheroids (Figure 2b). The total cargo of parasites inside the spheroids, which includes intracellular parasites, surface attached, as well as free parasites migrating inside spheroids through the ECM, was also higher on CL Brener than SylvioX10 infected spheroids (48% vs 18%, determined by qPCR; Figure 2d). Differences between strains were also registered when free-parasites (i.e., not associated to cells) inside spheroids were enumerated (Figure 2e,f). Altogether, these results evidence that both strains have different abilities to infect 3D cultures, being CL Brener strain 2–3 fold more infectious than SylvioX10. These findings were also registered with different multiplicity of infection, and contrast with

the similar behaviour of both strains on monolayer cultures (Figure S3). Of note, neither CFSE staining nor incubation for 24 altered the viability of trymomastigotes or their ability to infect cells (Figure S4).

2.2 | SylvioX10 and CL Brener trypomastigotes disseminate differentially inside spheroids

A panoramic view of spheroids, reconstructed from confocal stacks shows that SylvioX10 trypomastigotes were preferentially localised at the spheroid surface. Parasites were mostly focalized in large clumps that resembled a "patch-like" distribution pattern (Figure 3a, Movie S1). By contrast, CL Brener parasites were evenly distributed all over the surface of spheroids (Figure 3b, Movie S2).

The transmigration and invasiveness of trypomastigotes was analysed by scanning the spheroids by confocal microscopy. Most SylvioX10 trypomastigotes were retained at spheroid surface or at the first layers of cells, and only scarce trypomastigotes were detected up to 30 μm in depth (Figure 3c). On the other hand, CL Brener parasites were able to deepen into spheroids: migrated uniformly and were easily detected up to 50 μm in depth (Figure 3d). The migration through the spheroid seems to be a fast movement because similar patterns were observed from 1 h post infection (Figure S5). In brief, confocal scanning evidenced that CL Brener trypomastigotes can efficiently transmigrate deeply into spheroids, while SylvioX10 is retained at the surface, which corresponds with the differential virulence of both strains.

2.3 | CL Brener can use a paracellular migration route to move inside spheroids

To answer how trypomastigotes spread within spheroids, we analysed the parasite-spheroid interaction with higher resolution techniques, such as scanning electron microscopy (SEM) and higher power snapshots by confocal microscopy.

As evidenced by confocal microscopy, SEM images also showed numerous SylvioX10 parasites attached to the surface of individual cells (Figure 4A, panels b, c; white arrows). Notably, CL Brener trypomastigotes were predominantly caught entering into spheroids through the space between cell–cell junctions (Figure 4A, panels e, f; white asterisks). Spheroids infected with SylvioX10 also presented multiple intracellular amastigotes in the superficial layers—first 10 μm—of cells with an untidy distribution (Figure 4B panels a–c; 4C and Movie S3). Confocal slices of spheroids infected with CL Brener made evident that there is an orderly distribution pattern around cell–cell contacts (Figure 4B panels d–f; white asterisks). At shorter times, CL Brener trypomastigotes were plainly observed in the space between cells, on their way through the ECM, suggesting a paracellular route of transmigration within the spheroid (Figure 4d and movies S4 and S5). CL Brener trypomastigotes were also detected intracellularly, though fastened to the cellular membrane (movie S6).

2.4 | The capacity of transmigration is not transferable between strains

CL Brener and SylvioX10 strains presented not only dissimilar invasiveness profiles, but also their allocation at the superficial layers of spheroids was very distinctive (Figures 3 and 4). We then investigated if transmigration could be transferred from the highly migrant CL Brener strain to the low migrant SylvioX10, through soluble or secreted factors or by co-cultivation of both strains (Figure 5). Interestingly, each strain retained its own dissemination pattern (Figure 5A) and rate of infection (Figure 5B) irrespective of the presence (or absence) of the other strain. CM (including both soluble and vesicle-contained secreted factors) from CL Brener or SylvioX10 did not cause changes in the invasiveness pattern or percentage of infected cells (Figure S6). Together, these results indicate that the transmigration capacity of *T. cruzi* is a strain-specific trait that cannot be transferable by soluble or secreted factors, nor through co-cultivation of migrant and non-migrant trypomastigotes.

2.5 | Transmigration deep inside spheroids can be linked to virulence

To evaluate if the differential transmigration profile could be linked to parasite DTU or virulence, the transmigration into spheroids of other well characterised *T. cruzi* strains was also analysed. Low virulent strains (K98 and Dm28; TcI) presented low ability to transmigrate into spheroids (Figure 6). In contrast, virulent strains (RA [TcVI] and Y [TcII]) showed a transmigration pattern resembling the observed for CL Brener (Figure 6 and movies S7 and movies S8). Virulence of the strains is defined as the ability of a *T. cruzi* strain or clone to produce a lethal infection in mice. For non-lethal strains/clones the elapsed time from the initial infection to the appearance of bloodstream parasites and the level of parasites at the peak of parasitemia are also considered to determine the level of virulence (Figure S7).

Finally, we analysed the transmigration of four recent clinical isolates of *T. cruzi*. One isolate was derived from a *T. cruzi*-infected mother that after several pregnancies never delivered an infected child (isolate 773MM, TcI; non-congenital transmission). The other isolates, derived from babies that were born congenitally infected (isolates 173BB, TcI; 748BB, TcV; and 401BB, TcV; congenital transmission) (Volta et al., 2016). The non-congenital isolate (733MM) showed a low ability to migrate deep inside spheroids. Also, a "patch-like" distribution pattern, similar to the observed with SylvioX10 strain was observed (Figure 7b). In contrast, congenitally isolated parasites presented a highly migrant phenotype. Either DTU TcI or TcV isolates from congenitally infected babies were found deeply inside spheroids and easily visualised along the first 50 μm in depth (Figure 7a).

The cellular infection produced by 733MM was ~20%, a value near the one registered with the low virulent SylvioX10 strain, while the 40% of infection of cells in spheroids produced by congenital

isolates resembled the infection produced by CL Brener strain (Figure 7c).

Ultimately, because trypomastigotes of different strains behave differently when they are allowed to swim freely in the medium, we analysed parasite motility as a possible trait linked to invasiveness within spheroids (Figure S8). We consider a strain (or isolate) as poor motile when more than 20% of the parasites remain at the pellet in this assay. Although the swimming ability of SylvioX10 and CL Brener strains were considerably different and agree with their behaviour in spheroids, other strains showed no association between the transmigration inside spheroids and their swimming ability (for example, up to 60% of parasites from 173BB and 401BB—congenital isolates highly migrant in spheroids—remained between the pellet and layer 1).

3 | DISCUSSION

The infection with the protozoan parasite *T. cruzi* evolves from a short acute to a long lasting chronic phase when cardiac, neurological or intestinal disorders become evident (Rassi et al., 2010). Although the pathology appears only at the chronic phase, the infection of tissues initiates during acute phase and is the consequence of the early dissemination of trypomastigotes. Indeed, *T. cruzi* can disseminate and establish an intracellular infection in any tissue of the mammalian host (Costa et al., 2018). To accomplish this, trypomastigotes must migrate and actively cross several biological barriers, from the initial infection site to the target organs of damage, where parasites replicate intracellularly as amastigotes (Andrade & Andrews, 2005). Murine experimental models of *T. cruzi* infection have helped to understand that some parasite strains present tropism for certain tissues or organs while others are essentially pantropic and can colonise indistinctly any tissue (Costa et al., 2018; Lewis, Francisco, Taylor, & Kelly, 2015; Santi-Rocca et al., 2019). Usually, pantropic strains are more virulent in the murine model. It can be inferred that, since those strains colonise a broader range of tissues, they are also more efficient in the transmigration process. However, how trypomastigotes transmigrate, the mechanisms underlying this process and its significance in the host–parasite interplay are poorly understood.

In this work, we employed 3D cultures to mimic the tissular microarchitecture encountered by trypomastigotes in the mammalian host during its *in vivo* life cycle. We studied the process of transmigration and dissemination of the parasites across spheroids for the first time, and demonstrate a link between 3D transmigration and *in vivo* behaviour. Strains or isolates that are more virulent *in vivo* (in natural or experimental infections) transmigrated deeper inside spheroids than no virulent strains. In an *in vivo* infection, the ability to transmigrate will favour pathogen dissemination into the host, at the same time that parasites evade the immune system and increase the opportunity to find an adequate microenvironment to settle for the tissular infection (Drewry & Sibley, 2019; Harker, Ueno, & Lodoen, 2015; Kumar & Tolia, 2019; Lambert & Barragan, 2010). We have chosen Hela cells to begin our studies with spheroids because of its epithelial origin and because this lineage is usually employed in 2D monolayer cultures of *T. cruzi* (Castro-Gomes, Corrotte, Tam, & Andrews, 2016; Rodrigues et al., 2019; Schenkman & Mortara, 1992). Besides, with all its limitations, this 3D model certainly recreates much more similarly an *in vivo* microenvironment than 2D cultures. However, we are aware that invasiveness of trypomastigotes through microtissues should be dependent not only on the parasite strain but also on the cellular type employed to build spheroids. Indeed, preliminary assays with spheroids of HEK cells (epithelial lineage) depicted that CL Brener and Sylvio trypomastigotes behave as in Hela spheroids. On the contrary, Vero or HFF cells (that belong to fibroblastic lineages) rendered very compact spheroids, in which neither Sylvio nor CL Brener parasites are able to transmigrate. The reduction of oxygen and nutrients availability follows a gradient from 200 to 500 μm through the central zone of spheroids, where a necrotic center is established at sizes >500 μm (Hirschhaeuser et al., 2010). In our model, although spheroids have a size of 400 μm of diameter, the deepest point at which we have analysed parasite transmigration was 50 μm, at which nutrients are still available and is not a necrotic zone.

By employing the 3D spheroid model, we focused on one hand in the ability of *T. cruzi* strains to infect mammalian cells (evaluated by flow cytometry as cells with either internalised or attached parasites). On the other hand, we also examined the invasiveness of trypomastigotes, which means how deep inside the spheroids trypomastigotes are detected. Somehow both events (invasiveness and infection) are linked by the fact that *T. cruzi* strains that were highly migrant were also those that presented higher infection rates, probably because the transmigration was a necessary step to infect the cells located deep inside the spheroids. This fact can also explain why poorly migrant strains presented low infection rates in the 3D model, irrespective of their accurate infection rate in conventional 2D monolayer cultures. However, considering the times at which transmigration was analysed, it is unlikely that transmigration was the result of cellular invasion and replication of parasites. We postulate the transcellular and paracellular transmigration routes as two possible ways for trypomastigotes to reach the deeper layers of spheroids. Even more, we speculate that how *T. cruzi* transmigrates can be also a strain dependent trait and that different strains or isolates can employ differential transmigration strategies. Electronic microscopy images strongly suggest that CL Brener strain goes through spheroids by a paracellular route, without crossing the cells but between cell–cell junctions. Although the biological significance of this transmigration strategy should be carefully studied, we hypothesize that the paracellular route would allow the parasite to internalise into the tissues without disrupting the cellular homeostasis and, therefore, without triggering an inflammatory response. Moreover, a paracellular route would be a faster transmigration mechanism for trypomastigotes to find their target allocation inside tissues, without the need to invade and replicate intracellularly. In line with these results, Coates et al. (2013) showed that *T. cruzi* trypomastigotes can cross a monolayer of endothelial cells without cell damage. They suggested that this process might be mediated by the protease cruzipain, which can

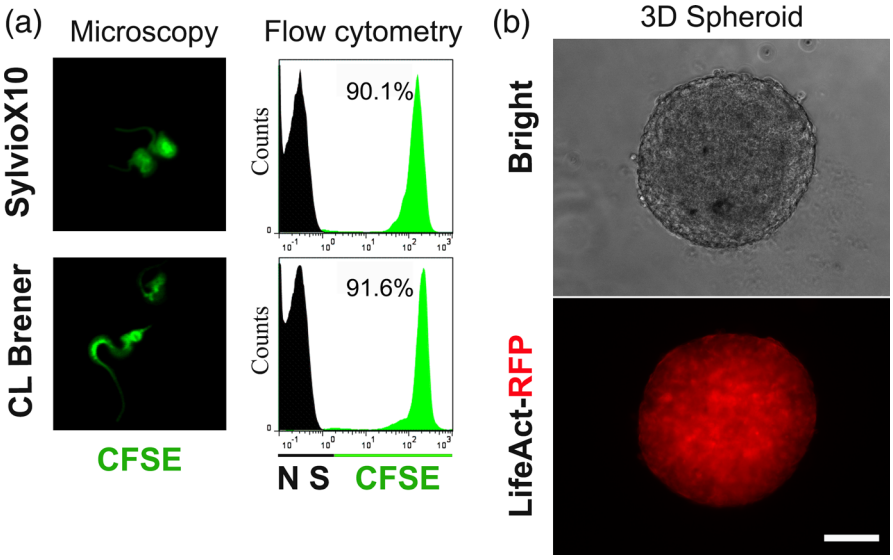

FIGURE 1 *Trypanosoma cruzi*—spheroids interaction: model setup. *T. cruzi* SylvioX10 (DTU TcI) and CL Brener (DTU TcVI) trypomastigotes were labelled with CFSE: fluorescent images (left panel) and quantification by flow cytometry (right panel). Black histograms: non labelled parasites; green histograms: CFSE labelled parasites. NS, negative staining. (b) Spheroid of HeLaR2 cells at 72 h post seeding. Scale bar = 100 μm

convert kininogen to bradykinin (involved in endothelial permeability) (Coates et al., 2013). The picture of trypomastigotes distribution was very distinctive between CL Brener and SylvioX10 strains, even from the initial steps of interaction with mammalian cells in our 3D model. While CL Brener trypomastigotes are regularly distributed and positioned in between cell–cell junctions on the external layers of the spheroid surface, SylvioX10 trypomastigotes are grouped in patches of several parasites stuck over the cells. Previous works with *Trypanosoma brucei* evidenced that trypomastigotes can cross the blood brain barrier both by transcellular and paracellular routes, promoting the expression of ICAM-1 and VCAM-1 (Grab et al., 2004; Mulenga, Mhlanga, Kristensson, & Robertson, 2001; Nikolskaia et al., 2006). On the other hand, *T. gondii* employs a paracellular route for tissue transmigration, through the interaction between TgMIC2 and host occludins from TJs and ICAM-1 (Barragan, Brossier, & Sibley, 2005; Weight, Jones, Horn, Wellner, & Carding, 2015). Interference with the transmigration process avoids *in vivo* infectivity both in *T. gondii* and *P. falciparum* (Huynh & Carruthers, 2006; Yang et al., 2017). Interestingly, the loss of genes associated with transmigration in *P. falciparum* did not impair cellular invasion, supporting the idea that tissue invasiveness and cellular infection can be two independent processes (Yang et al., 2017).

Trypomastigote's motility can be understood as its ability to present a directional movement, which in turn could impact on the cellular infection rates. We found a pronounced difference in swimming motility between SylvioX10 (low migrant and low motile) and CL Brener (high migrant and high motile) trypomastigotes. However, analyses of a broader panel of strains demonstrated that transmigration cannot be solely explained by the motile ability of trypomastigotes. Presumably, transmigration depends both on motility and migration of the parasite as well as on its interaction with the surrounding microenvironment. In this sense, Barragan and Sibley (2002) showed that a high migration rate of *T. gondii* is associated with a highly virulent phenotype (Barragan & Sibley, 2002). Indeed, correlation between high virulent strains and congenital toxoplasmosis has also been noted (Fuentes, Rubio, Ramirez, & Alvar, 2001; Howe & Sibley, 1995). On the other hand, Dóró et al. (2019) have very recently evaluated the migration of trypomastigotes of *T. carassii* in an *in vivo* model. This work clearly shows that the movement of parasites inside zebrafish occurs through the interstitial space and how its density and compaction determines the direction of trypomastigotes migration (Dóró et al., 2019).

During congenital transmission of *T. cruzi* infection, trypomastigotes must cross epithelial and connective tissues that compose the placental barrier to gain access to and infect the fetus. Therefore, transplacental infection is another aspect of *T. cruzi*-host interplay that is associated with parasite transmigration. We have characterised the invasiveness inside spheroids of isolates recently obtained from babies born with congenital Chagas disease. We demonstrated that the congenital isolates were highly invasive into spheroids, in contrast with the isolate obtained from a mother, which after delivered several children never transmitted the infection to her offspring, which showed a low/moderate transmigration ability. *T. cruzi* congenital transmission is the result of a complex interaction between trypomastigotes and the placental barrier (Bustos et al., 2019; Castillo et al., 2018; Juiz et al., 2018). Recently, Juiz et al. (2017) described a differential placental gene response induced by strains with different tropism and virulence. They reported that a strain that was isolated from a human case of congenital infection (VD) presented higher tropism by the murine placenta than a low-virulent and myotropic strain (K98) (Juiz et al., 2017). In our 3D model, K98 strain showed a low migrant phenotype. Although we did not analyse the transmigration profile of VD strain, all the congenital isolates assayed here were highly migrant.

The intratissular migration is key during the development of metastasis and it has been approached in several studies on cancer (Stuelten, Parent, & Montell, 2018). Tumoral cells produce and prompt to the secretion of cytokines and proteases that will favour the migration across different biological barriers. Proteases are necessary to disrupt cell–cell junctions, ECM and the basal lamina (Wolf & Friedl, 2011). Although little is known about the transmigration

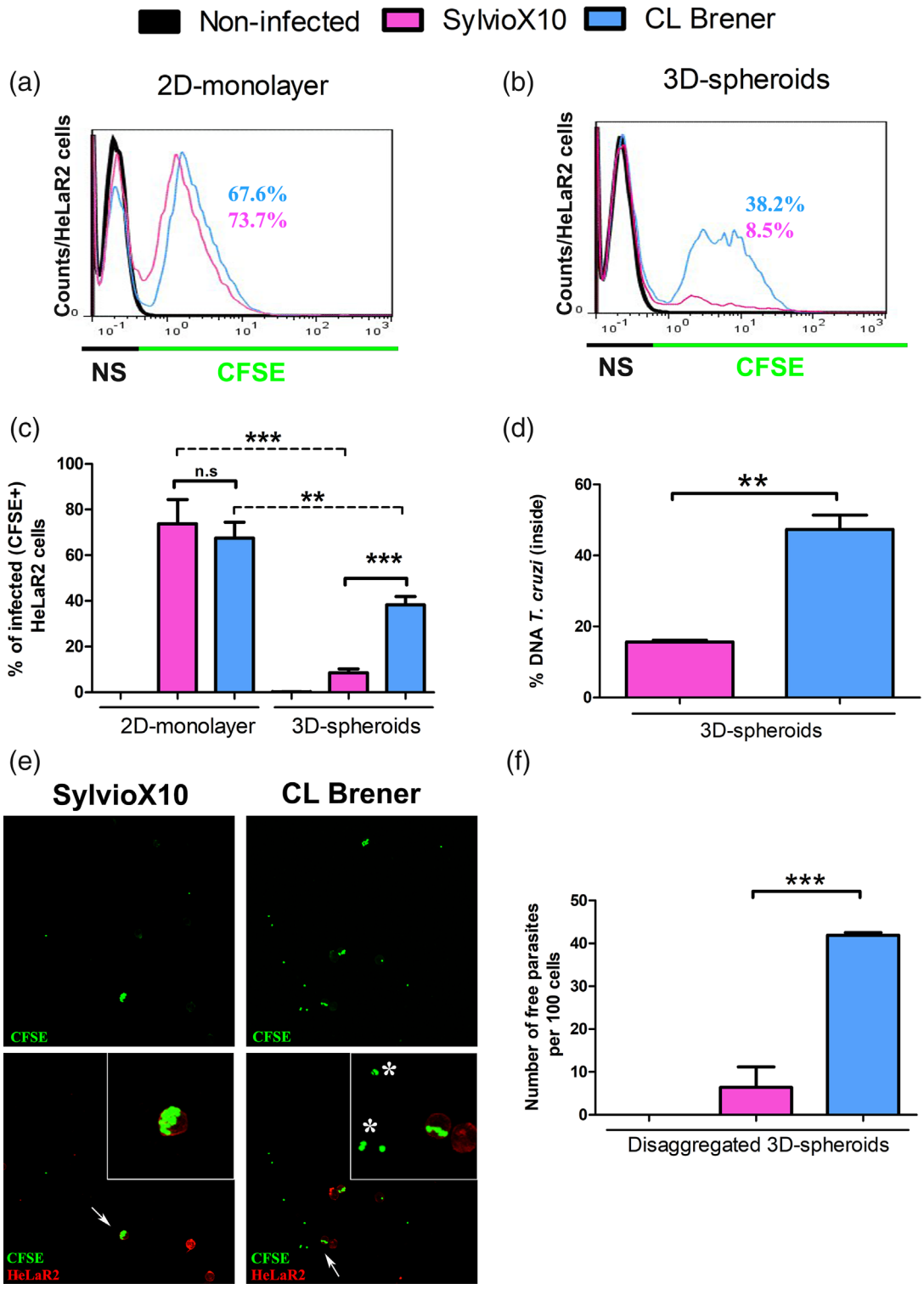

FIGURE 2 Trypomastigotes from virulent (CL Brener) and low-virulent (SylvioX10) strains show differential abilities to infect 3D-spheroid cultures. HeLaR2 (grown as monolayers or as spheroids, see Material and Methods section) were incubated with 10 m.o.i. of CFSE-labelled CL Brener or SylvioX10 trypomastigotes or non-infected (control). (a,b) At 24 h post infection, cells were trypsinized and the rate of infected HeLaR2 cells (either with internalised or attached parasites) was determined by flow cytometry. (c) Quantification of three independent experiments carried out as described for (a) and (b). (d) Quantification of the total parasite cargo inside spheroids, which includes both cell-associated parasites and free parasites inside spheroids from three independent experiments. At 24 h post infection either intact spheroids or the whole content of the well (intact spheroids plus culture media with non-internalised parasites) were harvested and total DNA purified. Parasite content was estimated on the basis of qPCR of a single copy *T. cruzi* gene (*PCD6*, TriTryp gene ID: TcCLB.507099.50). Percentage of *T. cruzi* DNA inside spheroids respect to total *T. cruzi* DNA in the well was calculated. (e) Free parasites inside spheroids infected with CL Brener or SylviX10, at 24 h p.i. Representative confocal images of disaggregated spheroids, white arrows: magnified cells; white asterisks: free parasites. (f) Quantification of free parasites released from disaggregated spheroids. Data expressed as number of free-parasites for each 100 HeLaR2 cells. Graphs represent the mean ± SD of three independent experiments. (c): one-way ANOVA followed by Bonferroni's multiple comparison test; (d and f): *t test*, $^{*}p < .05$, $^{**}p < .01$, $^{***}p < .001$

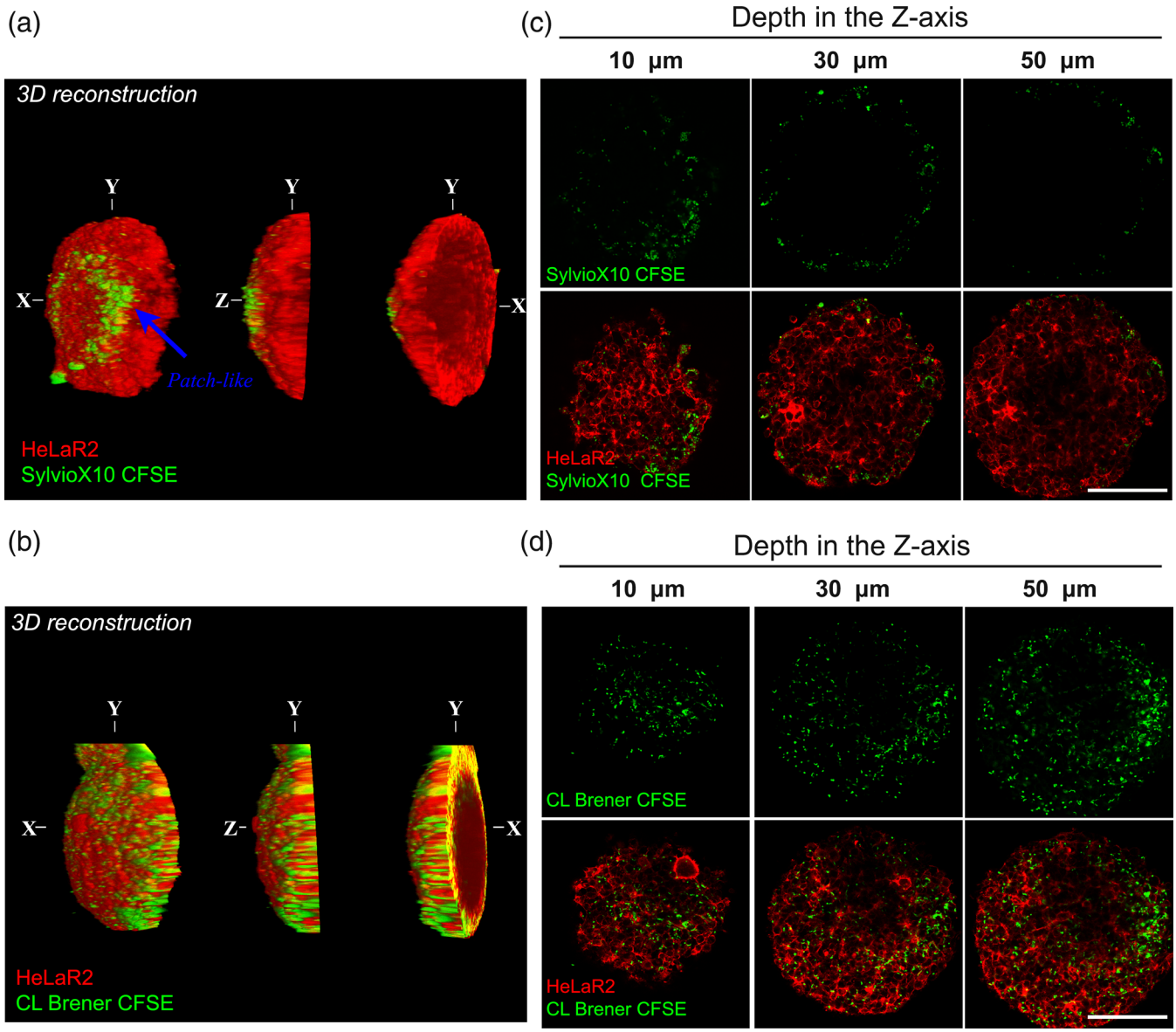

FIGURE 3 Transmigration profile of trypomastigotes from different strains within spheroids. (a and b). 3D reconstruction of HeLaR2 spheroids infected with CFSE-SylvioX10 or CFSE-CL Brener trypomastigotes. Z-stack images were obtained by confocal microscopy. The distribution on the surface (X-Y left image), the side plane (Z-Y middle image) and inside the spheroid (Y-X right image, transversal view) are shown. Green: CFSE-trypomastigotes. Red: LifeAct-RFP of HeLa cells. (C and D) Representative images of three confocal planes obtained at 10, 30 and 50 µm in depth on the *z* axis (40× objective). The detailed distribution pattern of parasites is observed—green fluorescence. Scale bar: 100 µm

process in host–pathogen interactions, the secretion of proteases could also be required to disrupt intercellular junctions and ECM for *T. cruzi* transmigration. However, in our experimental conditions, the invasiveness was not a transferable feature between strains, neither by soluble or secreted factors nor by co-cultivation of invasive and non-invasive trypomastigotes. This observation suggests that unsecreted and strain specific factors are required to transmigrate into the spheroids, while it does not exclude the involvement of proteases and other soluble factors. Differentially-expressed and/or strain specific membrane-associated molecules from trypomastigotes might be targets to be evaluated in the near future.

Altogether, our results demonstrated that in a 3D microenvironment each strain presents a characteristic migration pattern and tissular distribution that could be associated to their *in vivo* behaviour. Our work also validates the accuracy and utility of the 3D spheroid model to study complex host–parasite interactions. Certainly, the findings presented here could not have been studied with traditional 2D monolayer cultures.

4 | EXPERIMENTAL PROCEDURE

4.1 | Reagents and sera

Ultrapure Agarose, Carboxy-fluoresceinsuccinimidyl ester (CFSE) and CellTrace™ Far Red (CTFR) were acquired from Invitrogen.

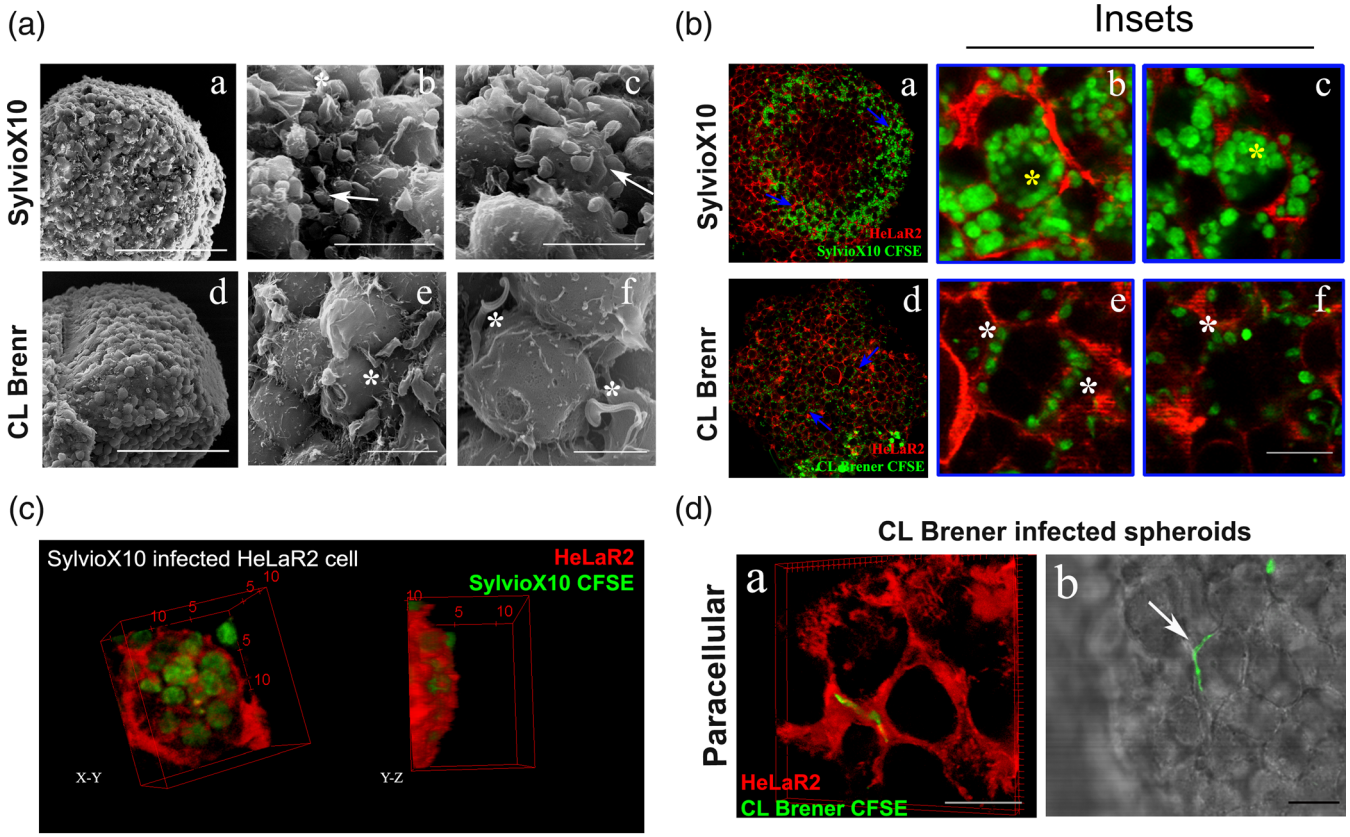

FIGURE 4 Host cell–parasite interaction pattern at the spheroid surface of different strains of *T. cruzi*. Spheroids were cultured with CFSE-SylvioX10 or CFSE-CL Brener. (A) Cell-parasite interaction on the surface of infected spheroids after 24 h of infection. SEM microscopy showing the whole surface of infected spheroids (images a and d) or detailed cell–parasite interactions (b-c for SylvioX10 and e-f for CL Brener) are shown. White arrows show groups of parasites on the surface of SylvioX10 infected spheroids. White asterisks show CL Brener parasites located in the site of cell cell–cell contact. Scale bar for a and d: 100 μm; b and c: 10 μm; d: 100 μm; e: 10 μm: f: 5 μm. (B) Confocal microscopy capturing cell infection at 10 μm of infected spheroids with 60× objective. The distribution pattern of parasites on the surface of infected spheroids is observed in a and d images for SylvioX10 and CL Brener, respectively. Blue arrows show magnified insets (b-c for SylvioX10 and e-f for CL Brener). Yellow asterisks show multi-infected cells. White asterisks show cell–cell contact associated parasites. Scale bar = 15 μm. (C) Multi-infected cell on the surface of SylvioX10 infected spheroids was reconstructed in 3D. Multiple intracellular amastigotes can be observed. (D) Spheroids of HeLaR2 cells were incubated with CFSE-CL Brener trypomastigotes for 1 h and then photographed by confocal microscopy. CFSE-trypomastigotes in the paracellular space both in fluorescence images (a) as well as in bright light (b) are shown. Scale bar 15 μm

Polyethylenimine (PolyAr87-PEI) transfection reagent was obtained from Facultad de Farmacia y Bioquímica (University of Buenos Aires). Anti *T. cruzi* antisera developed in mice was generated in our laboratory and used along with goat anti-mouse conjugated to Alexa-488 or Alexa-647 (Molecular Probes).

4.2 | Ethical statement

All protocols conducted with animals were designed and carried out in accordance with international ethical standards for animal experimentation (Helsinki Declaration and its amendments, Amsterdam Protocol of welfare and animal protection and National Institutes of Health, USA NIH, guidelines) and were approved by the Institutional Animal-Care Ethics Committee of the University of San Martin (CICUAE, protocol number: 15/2019).

4.3 | Parasites and conditioned media

T. cruzi trypomastigotes from different strains and discrete typing units (DTUs) employed were: SylvioX10, K98, Dm28, 193-733MM and 199-173BB (DTU TcI); Y (DTU TcII); 185-748BB and 186-401BB (DTU TcV) and RA and CL Brener (DTU TcVI). All strains were DNA genotyped by PCR-RFLP of *TcSC5D* and *TcMK* genes (Figure S1), as described (Cosentino & Agüero, 2012). Trypomastigotes of 193-733MM, 199-173BB, 185-748BB and 186-401BB are recent *T. cruzi* isolates (Volta et al., 2016). The SylvioX10 employed is the clone SyvioX10/IIB, derived from SylvioX10/7 that lost its virulent phenotype (Postan, Dvorak, & McDaniel, 1983). CL Brener is also a clone and K98 a clone derived from the CA-I strain (Celentano & González Cappa, 1992). On the other hand, RA (González Cappa, Bijovsky, Freilij, Muller, & Katzin, 1981), Dm28 and Y are well characterised *T. cruzi* strains that present homogenous behaviour.

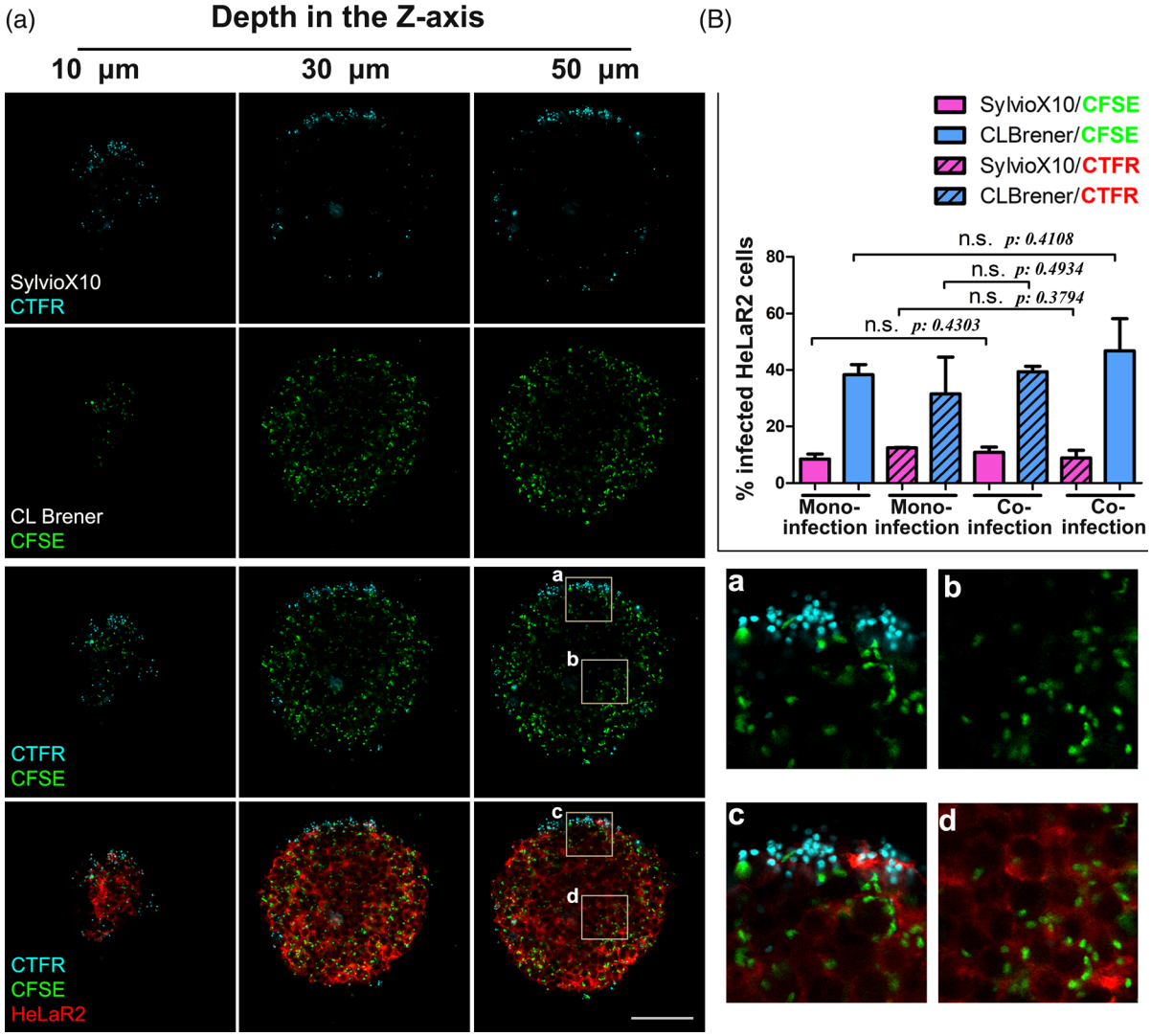

FIGURE 5 Invasiveness within spheroid is an intrinsic feature of each strain, not complemented in trans. Spheroids of HeLaR2 cells were incubated with CFSE-CL Brener, CTFR-CL Brener, CFSE-SylvioX10 or CTFR-SylvioX10 or simultaneously co-incubated with both strains labelled with different dyes. (A) Representatives images of three confocal planes obtained at 10, 30 and 50 µm in depth—on the *z* axis—with a 40× objective. Cyan: CTFR-SylvioX10; green: CFSE-CL Brener; red: HeLaR2 cells. Magnified insets (a-d) are shown in the right panels. Scale bar = 100 µm. (B) The same assay as described in A but spheroids were disaggregated and cells with either attached or internalised parasites were quantified by flow cytometry. Infections with one (mono-infections) or both strains simultaneously (co-infections) were carried out also with interchanged dyes. The percentage of infected cells was significantly different between SylvioX10 and CL Brener parasites in all conditions tested. On the other hand, no differences in the infection rate for each strain, both with the use of different staining dyes, as well as, during the mono infections versus the co-infections were observed. Graphs represent the mean ± SD of three independent experiments. Data were analysed by one-way ANOVA followed by Bonferroni's multiple comparison test

Parasites were routinely maintained by *in vitro* cultures on Vero cells as previously described (Bernabo et al., 2013), and trypomastigotes harvested from supernatants. For infection of mice, trypomastigotes were diluted with PBS-1%BSA at 2.5×10^6 par/ml and 0.1 ml were injected by intraperitoneal route. Animals were followed up for parasitemia and survival as previously described (Caeiro et al., 2018).

Culture-derived trypomastigotes were labelled with CellTrace™ CFSE (10 µM) as we previously described (Rodríguez et al., 2019). Trypomastigotes were alternatively labelled with CTFR (5 µM), essentially with the same protocol with slight differences in the incubation time (20 min at 37°C, followed by the addition of 1 ml of complete medium and an additional incubation of 5 min at 37°C in the dark). After labelling, the motility of parasites was controlled under light microscope. The percentage of labelled parasites and the fluorescence intensity of CFSE and CTFR was determined by flow cytometry.

T. cruzi derived conditioned medium (CM) was obtained by a previously standardised protocol (Caeiro et al., 2018). In brief, cell-derived trypomastigotes (100×10^6) were washed with PBS, resuspended in 1 ml of minimal essential medium (MEM) without serum (or MEM without parasites as control medium) and incubated for 6 h at 37°C in a 5% CO_2 humidified atmosphere. Then, parasites were pelleted by centrifugation and the cell-free supernatant

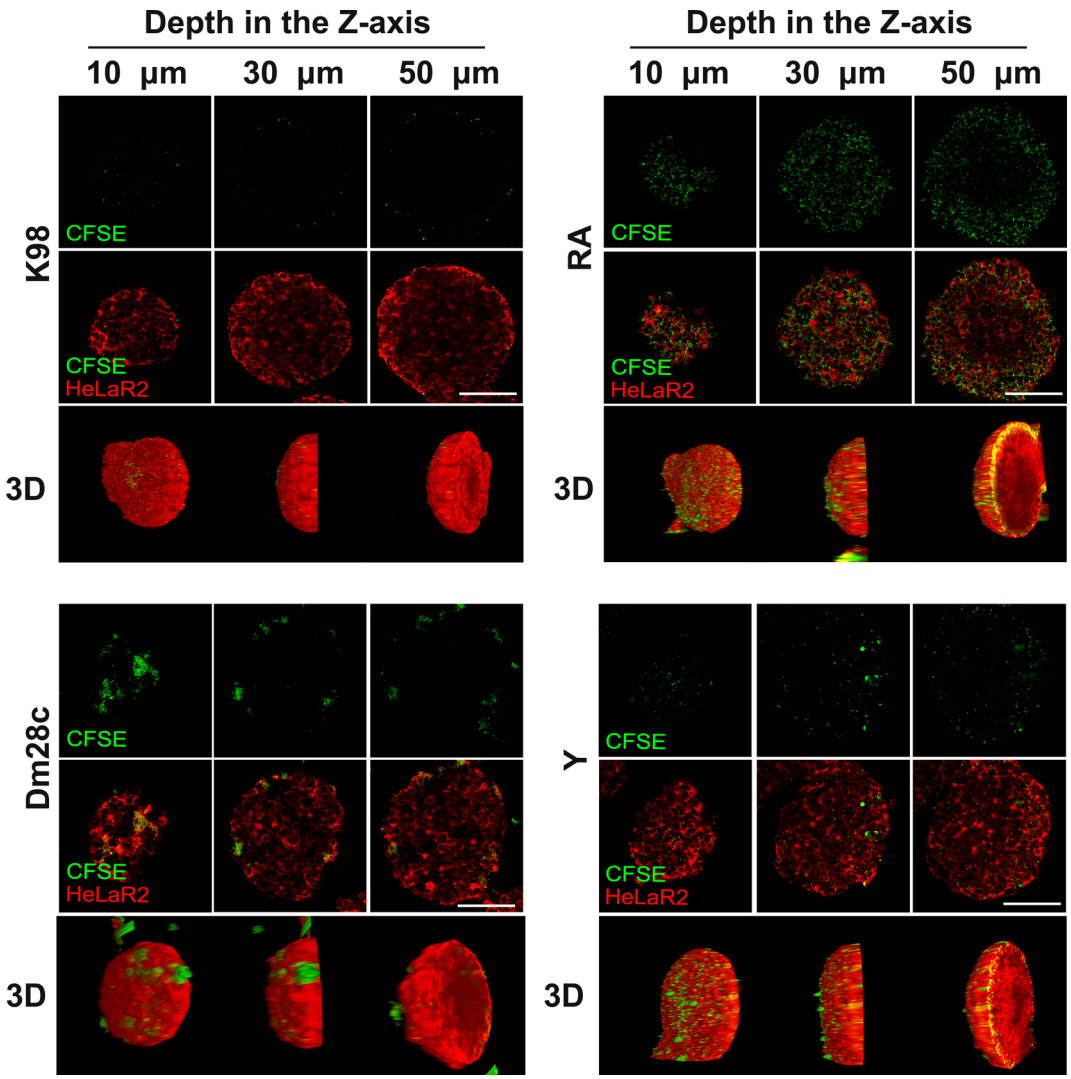

FIGURE 6 The capacity of dissemination is linked to virulence. Spheroids of HeLaR2 cells were incubated with K98, Dm28c, Y or RA strains for 24 h. Three confocal planes were obtained at 10, 30 and 50 µm in depth—on the *z* axis—with 40× objective. The detailed distribution pattern of parasites is observed. 3D-reconstruction is shown in lower panels. Green: CFSE labelled parasites. Red: LifeAct-RFP. Scale bar = 100 µm

(containing both extracellular vesicles as well as vesicle-free secreted material) was centrifuged twice for 10 min at 15,000×*g*. The clarified supernatant was filtered through a 0.45 µm syringe filter, to obtain the CM, which was aliquoted and stored at −70°C until use.

4.4 | Cell culture and stable HeLaR2 cell line generation

Vero, HeLa and HEK293T cells were grown in MEM (Gibco) supplemented with 10% (v/v) fetal bovine serum (Natocor), 100 U/ml penicillin and 10 µg/ml streptomycin. Cells were maintained at 37°C in 5% CO_2 and 95% air in a humidified incubator. To obtain Hela cells stably expressing LifeAct-RFP, permissive HEK293T cells were first employed to produce lentiviral particles packed with LifeAct-RFP, essentially as described by Gerber et al. (2015). Briefly, HEK293T were seeded on 24-well plates (3×10^4 cells/well) and transfected 24 h later by the PEI method with a mix of 0.5 µg pCMV-dR8.9 DVpr (packaging plasmid), 0.05 µg pCMV–VSV-G (envelope plasmid) and 0.5 µg of the pLenti LifeAct-RFP (transfer plasmid) per well. The supernatant containing lentiviral particles packed with LifeAct-RFP was collected at 48 and 72 h after transfection, precleared and concentrated by centrifugation. HeLa cells (3×10^4 cells/well) were transduced in MEM containing 10% FBS with a 0.3 m.o.i. of lentiviral particles, and expanded in culture flasks. Cells expressing LifeAct-RFP (HeLaR) were sorted by flow cytometry, and cloned by limiting dilution. The clone number 2 (HeLaR2) stably expressing LifeAct-RFP was selected and employed for all the experiments.

4.5 | HeLa spheroids and infection model

Spheroids of HeLaR2 cells were generated by the liquid overlay method (Carlsson & Yuhas, 1984). Cells (1,000/well) were added to U-bottom

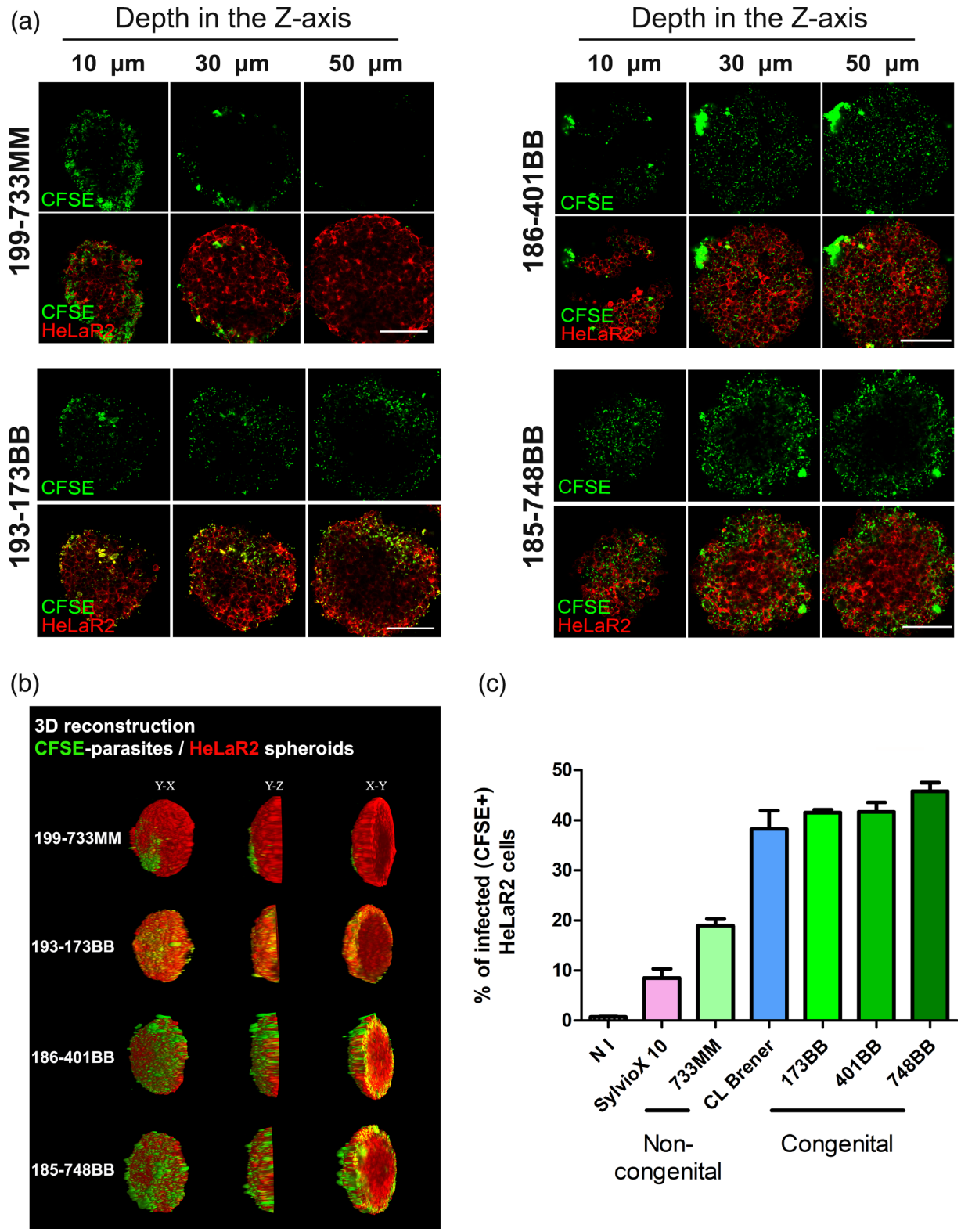

FIGURE 7 Congenital trypomastigotes are more invasive and infective than non-congenital parasites. Spheroids of HeLaR2 cells were incubated with 733MM, 173BB, 401BB or 748BB recent clinical isolates for 24 h. (a) Confocal planes were obtained at 10, 30 and 50 µm in depth—on the *z* axis—with 40× objective. The detailed distribution pattern of parasites is observed. Scale bar = 100 µm. (b) Three-D-reconstruction of infected spheroids with each strain is shown. Green: CFSE labelled parasites. Red: LifeAct-RFP. (c) Percentage of infected HeLaR2 cells to compare infectivity of non-congenial vs congenital isolated. Pink and blue bars show SylvioX10 and CL Brener % of infection, respectively, as comparison points. Graphs represent the mean ± SD of three independent experiments

96-well plates coated with agarose 1% in PBS (w/v) and cultured in MEM 10% FBS. The formation of spheroids was controlled by microscopy from 24 h post seeding (Figure S2). At 72 h, each well contained one spheroid of 300–400 μm diameter, conformed by ≃9,000 cells.

For *T. cruzi* infection, 12 spheroids were placed on each well of an agarose pre-coated p24 plate and incubated with 1 or 10 m.o.i. of trypomastigotes (or control medium) for 1 or 24 h, in MEM supplemented with 4% FBS. When appropriate, 100 μl of medium was replaced by 100 μl of CM. When indicated, 2D-monolayers of HeLaR2 cells (10×10^5 cells/well) were incubated with 1 or 10 m.o.i. of trypomastigotes also labelled with CFSE in a final volume of 500 μL of MEM 4%.

For co-infection assays, 12 spheroids (in one p24 well) were simultaneously incubated with CL Brener and SylvioX10 for 24 h with 10 m.o.i. of each *T. cruzi* strain, labelled with a different stain.

4.6 | Cellular infection determined by flow cytometry

Infected spheroids were collected in 1.5 ml tubes, washed three times with PBS and disaggregated by addition of 200 μl 0.25% trypsin/EDTA for 10 min at 37°C. The cellular pellet—collected by centrifugation 10 min at 1,000×*g*—was washed three times and fixed in PBS 0.5% PFA. Infected 2D-monolayer cells were trypsinized and treated like 3D spheroids. Samples were acquired on a FACSCalibur (Becton Dickinson); gated HeLaR2 by forward and side scatter parameters were selected. A total of 10,000 events were analysed for each condition. FL1− cells represented uninfected HeLaR2 cells while FL1+ represented cells infected (either with intracellular parasites and/or attached to cell membrane) with CFSE-labelled parasites, FL4+ cells were those infected with CTFR-labelled parasites. Data was analysed using FlowJo v10.0.7 software. Statistical significance was determined by two-tailed unpaired student *t test* (Prism, GraphPad Software).

4.7 | Quantification of free-parasites inside spheroids

Infected spheroids disaggregated by trypsin treatment were centrifuged for 10 min at 5,700×*g* to collect HeLaR2 cells and parasites that were infecting or attached to HeLa cells, as well as parasites that were free inside spheroids (i.e., not associated to cells but inside spheroids). The pellet was then analysed by confocal microscopy to determine infected cells as well as free parasites (expressed as number of free-parasites for each 100 HeLaR2 cells). Statistical significance was determined by two-tailed unpaired student *t test* (Prism, GraphPad Software).

4.8 | Parasitic load into spheroids

The total cargo of parasites inside the spheroids, either infecting cells or free in the ECM, was determined by qPCR. For doing so, each treatment was carried out by duplicate: one sample was used to determine the parasite load associated to spheroids (sample 1) while the other was used to determine the total cargo of parasites in the well (sample 2: parasites associated to spheroids plus parasites free in the medium/well). Infection was carried out as mentioned above. After 24 h, spheroids from sample 1 were collected in 1.5 ml tubes and carefully washed five times with sterile PBS to eliminate parasites from the supernatant avoiding the disassembling of spheroids. Instead, for sample 2 spheroids and medium were collected together, centrifuged for 10 min at 5700×*g* and the pellet washed with sterile PBS. Samples were subjected to a standard salting out protocol to obtain genomic DNA (Miller, Dykes, & Polesky, 1988). gDNA concentration was measured using Nanodrop and 50 ng were used in each qPCR reaction, which were carried out with Kapa Sybr Fast Universal Kit (Biosystems) in a 7500 Real Time PCR System (Applied Biosystems). The *T. cruzi* single copy gene *PCD6* (TcCLB.507099.50) was amplified with primers v099.50bFw (CAGGCATCACCGTATTTTCCA) and 099.50bRev (CTCTTGTTCCGTGCCAAACA) (Campo, 2017). To determine *T. cruzi* DNA (*Tc*DNA) abundance, DNA content was normalised to human *GAPDH* gene (53MFZ-GAPDHFw: ACCACCCTGTTGCTGTAGCCAAAT and 54MFZRev: GACCTGACCTGCCGTCTAGAAAAA). Results were analysed with the LinReg software (Ramakers, Ruijter, Deprez, & Moorman, 2003). The percentage of *Tc*DNA inside spheroids was calculated as *X*% = *Tc*DNAsample1 × 100/*Tc*DNAsample2 and expressed as mean ± SD of three independent experiments. Statistical significance was determined by student *t test* (GraphPad software).

4.9 | Parasite invasiveness and dissemination

Infected spheroids were fixed by adding PFA to a 3.2% final concentration and incubated at 37°C for 1.5 h. Then, spheroids were washed with PBS as described previously (Rodríguez et al., 2019) and mounted. Fluorescence images were acquired with a confocal Olympus FV1000 microscope. CFSE or CTFR labelled parasites were imaged with a 488 nm or 647 nm laser, respectively, while HeLaR2 cells were imaged at 530 nm. Z-stacks were collected with a 10× objective from 0 to 150 μm in depth with 2 μm intervals in the vertical *z*-axis. Alternatively, images were acquired with a 40× objective, and the spheroid was scanned at 10, 30 and 50 μm in depth from the surface. To determine the localization of parasites, spheroids were analysed with a 60× objective and Z-stacks were collected at 0.2 μm intervals in the *z*-axis. All images were analysed with ImageJ (Schneider, Rasband, & Eliceiri, 2012) software; 3D reconstructions and 3D-movies were generated with the 3D-viewer plugin.

4.10 | Electron microscopy

Infected spheroids were fixed in 4% PFA and serially dehydrated with increasing ethanol solutions (10–100%) followed by critical point drying with carbon dioxide. Samples were then coated with 60%/40%

palladium/gold and acquired with a scanning electron microscope (Philips—XL Serie 30).

4.11 | Free-swimming assay

Trypomastigotes (15×10^6) were resuspended in 5 ml MEM 4% SFB, transferred to round-bottom centrifuge tubes (Oak Ridge Style) and centrifuged at 2,500×*g* for 8 min, which resulted in parasites at the bottom of the tubes forming a thin pellet. The tubes were then incubated 2 h at 37°C, to allow trypomastigotes to freely swim. Aliquots of 1 ml were carefully taken from the top (layer 5) to the bottom; the pellet was resuspended in 1 ml of medium. Parasites in each fraction were enumerated by counting in a Neubauer chamber.

4.12 | Statistical analysis

All statistical analyses and graphs were performed with GraphPad Prism 7 (GraphPad Software, USA). We used a two-tailed unpaired *t test* when the means of two groups were compared. When more than two groups were compared, we used one-way ANOVA with Bonferroni multiple comparison test. Significant differences were designed when *p*-value (*p*) n.s. ≥.05, $^*p < .05$, $^{**}p < .01$, $^{***}p < .001$.

ACKNOWLEDGEMENTS

We acknowledge L. Sferco and A. Chidichimo for technical assistance with *in vitro* parasite cultures, and V. Campo and G.V. Levy for advice in qPCR assays. We are grateful to A.M.M. Massaldi for checking the English version of the manuscript. This work was supported by grants from Agencia Nacional de Promoción Científica y Tecnológica/Fondo para la Investigación Científica y Tecnológica—ANPCyT/FONCyT—(PICT-2016-0108 to VT and PICT 2017-2644 to MER) from Argentina. The funders had no role in study design, data collection and analysis, decision to publish, or preparation of the manuscript.

CONFLICT OF INTEREST

The authors declare no potential conflict of interest.

AUTHOR CONTRIBUTIONS

Conceived and designed the experiments: V.T., M.E.R. Performed the experiments: M.E.R., M.R., L.D.C., Y.E.M. Analysed the data: M.E.R., M.R., L.D.C., Y.E.M., D.O.S., V.T. Contributed reagents/materials/analysis tools: A.P., D.O.S., J.B. Wrote the paper: M.E.R., V.T. Supervised the project: V.T. Funding acquisition: M.E.R., V.T. All authors provided critical feedback and helped shape the research, analysis and manuscript.

ORCID

Valeria Tekiel https://orcid.org/0000-0003-2981-2312

REFERENCES

Andrade, L. O., & Andrews, N. W. (2005). Opinion: The *Trypanosoma cruzi*–host-cell interplay: Location, invasion, retention. *Nature Reviews Microbiology*, *3*(10), 819–823. https://doi.org/10.1038/nrmicro1249

Barragan, A., Brossier, F., & Sibley, L. D. (2005). Transepithelial migration of *Toxoplasma gondii* involves an interaction of intercellular adhesion molecule 1 (ICAM-1) with the parasite adhesin MIC2. *Cellular Microbiology*, *7*(4), 561–568. https://doi.org/10.1111/j.1462-5822.2005.00486.x

Barragan, A., & Sibley, L. D. (2002). Transepithelial migration of *Toxoplasma gondii* is linked to parasite motility and virulence. *The Journal of Experimental Medicine*, *195*(12), 1625–1633. https://doi.org/10.1084/jem.20020258

Baruzzi, A., Remelli, S., Lorenzetto, E., Sega, M., Chignola, R., & Berton, G. (2015). Sos1 regulates macrophage Podosome assembly and macrophage invasive capacity. *The Journal of Immunology*, *195*(10), 4900–4912. https://doi.org/10.4049/jimmunol.1500579

Belew, A. T., Junqueira, C., Rodrigues-Luiz, G. F., Valente, B. M., Oliveira, A. E. R., Polidoro, R. B., & Teixeira, S. M. R. (2017). Comparative transcriptome profiling of virulent and non-virulent *Trypanosoma cruzi* underlines the role of surface proteins during infection. *PLoS Pathogens*, *13*(12), e1006767. https://doi.org/10.1371/journal.ppat.1006767

Bernabo, G., Levy, G., Ziliani, M., Caeiro, L. D., Sanchez, D. O., & Tekiel, V. (2013). TcTASV-C, a protein family in *Trypanosoma cruzi* that is predominantly Trypomastigote-stage specific and secreted to the medium. *PLoS One*, *8*(7), e71192. https://doi.org/10.1371/journal.pone.0071192

Bustos, P. L., Milduberger, N., Volta, B. J., Perrone, A. E., Laucella, S. A., & Bua, J. (2019). *Trypanosoma cruzi* infection at the maternal-fetal Interface: Implications of parasite load in the congenital transmission and challenges in the diagnosis of infected newborns. *Frontiers in Microbiology*, *10*, *1250*. https://doi.org/10.3389/fmicb.2019.01250

Caeiro, L. D., Alba-Soto, C. D., Rizzi, M., Solana, M. E., Rodriguez, G., Chidichimo, A. M., & Tekiel, V. (2018). The protein family TcTASV-C is a novel *Trypanosoma cruzi* virulence factor secreted in extracellular vesicles by trypomastigotes and highly expressed in bloodstream forms. *PLoS Neglected Tropical Diseases*, *12*(5), e0006475. https://doi.org/10.1371/journal.pntd.0006475

Campo, V. A. (2017). Comparative effects of histone deacetylases inhibitors and resveratrol on *Trypanosoma cruzi* replication, differentiation, infectivity and gene expression. *International Journal for Parasitology: Drugs and Drug Resistance*, *7*(1), 23–33. https://doi.org/10.1016/j.ijpddr.2016.12.003

Carlsson, J., & Yuhas, J. M. (1984). Liquid-overlay culture of cellular spheroids. Recent results in cancer research. *Fortschritte Der Krebsforschung. Progrès Dans les Recherches Sur Le Cancer*, *95*, 1–23. https://doi.org/10.1007/978-3-642-82340-4_1

Castillo, C., Carrillo, I., Libisch, G., Juiz, N., Schijman, A., Robello, C., & Kemmerling, U. (2018). Host-parasite interaction: Changes in human placental gene expression induced by *Trypanosoma cruzi*. *Parasites & Vectors*, *11*(1), 479. https://doi.org/10.1186/s13071-018-2988-0

Castro-Gomes, T., Corrotte, M., Tam, C., & Andrews, N. W. (2016). Plasma membrane repair is regulated extracellularly by proteases released from lysosomes. *PLoS One*, *11*(3), e0152583.

Celentano, A. M., & González Cappa, S. M. (1992). Induction of macrophage activation and opsonizing antibodies by *Trypanosoma cruzi* subpopulations. *Parasite Immunology*, *14*(2), 155–167.

Coates, B. M., Sullivan, D. P., Makanji, M. Y., Du, N. Y., Olson, C. L., Muller, W. A., & Epting, C. L. (2013). Endothelial transmigration by *Trypanosoma cruzi*. *PLoS One*, *8*(12), e81187. https://doi.org/10.1371/journal.pone.0081187

Cosentino, R. O., & Agüero, F. (2012). A simple strain typing assay for *Trypanosoma cruzi:* Discrimination of major evolutionary lineages from

a single amplification product. *PLoS Neglected Tropical Diseases*, *6*(7), e1777. https://doi.org/10.1371/journal.pntd.0001777

Costa, F. C., Francisco, A. F., Jayawardhana, S., Calderano, S. G., Lewis, M. D., Olmo, F., & Taylor, M. C. (2018). Expanding the toolbox for *Trypanosoma cruzi*: A parasite line incorporating a bioluminescence-fluorescence dual reporter and streamlined CRISPR/Cas9 functionality for rapid *in vivo* localisation and phenotyping. *PLoS Neglected Tropical Diseases*, *12*(4), e0006388. https://doi.org/10.1371/journal.pntd.0006388

Dóró, É., Jacobs, S. H., Hammond, F. R., Schipper, H., Pieters, R. P., Carrington, M., & Forlenza, M. (2019). Visualizing trypanosomes in a vertebrate host reveals novel swimming behaviours, adaptations and attachment mechanisms. *eLife*, *8*, *e48388*. https://doi.org/10.7554/eLife.48388

Drewry, L. L., & Sibley, L. D. (2019). The hitchhiker's guide to parasite dissemination. *Cellular Microbiology*, *21*, e13070. https://doi.org/10.1111/cmi.13070

Fennema, E., Rivron, N., Rouwkema, J., van Blitterswijk, C., & de Boer, J. (2013). Spheroid culture as a tool for creating 3D complex tissues. *Trends in Biotechnology*, *31*(2), 108–115. https://doi.org/10.1016/J.TIBTECH.2012.12.003

Ferrão, P. M., Nisimura, L. M., Moreira, O. C., Land, M. G., Pereira, M. C., de Mendonça-Lima, L., & Garzoni, L. R. (2018). Inhibition of TGF-β pathway reverts extracellular matrix remodeling in *T. cruzi* infected cardiac spheroids. *Experimental Cell Research*, *362*(2), 260–267. https://doi.org/10.1016/j.yexcr.2017.11.026

Fuentes, I., Rubio, J. M., Ramirez, C., & Alvar, J. (2001). Genotypic characterization of *Toxoplasma gondii* strains associated with human toxoplasmosis in Spain: Direct analysis from clinical samples. *Journal of Clinical Microbiology*, *39*(4), 1566–1570. https://doi.org/10.1128/JCM.39.4.1566-1570.2001

Garzoni, L. R., Adesse, D., Soares, M. J., Rossi, M. I. D., Borojevic, R., & de Meirelles, M. de N. (2008). Fibrosis and hypertrophy induced by *Trypanosoma cruzi* in a three-dimensional cardiomyocyte-culture system. *The Journal of Infectious Diseases*, *197*(6), 906–915. https://doi.org/10.1086/528373

Gerber, P. P., Cabrini, M., Jancic, C., Paoletti, L., Banchio, C., von Bilderling, C., … Ostrowski, M. (2015). Rab27a controls HIV-1 assembly by regulating plasma membrane levels of phosphatidylinositol 4,5-bisphosphate. *The Journal of Cell Biology*, *209*(3), 435–452. https://doi.org/10.1083/jcb.201409082

Giannattasio, A., Weil, S., Kloess, S., Ansari, N., Stelzer, E. H. K., Cerwenka, A., & Koch, J. (2015). Cytotoxicity and infiltration of human NK cells in *in vivo*-like tumor spheroids. *BMC Cancer*, *15*(1), 351. https://doi.org/10.1186/s12885-015-1321-y

González Cappa, S. M., Bijovsky, A. T., Freilij, H., Muller, L., & Katzin, A. M. (1981). Isolation of a *Trypanosoma cruzi* strain of predominantly slender form in Argentina. *Medicina (B Aires).*, *41*(1), 119–120.

Grab, D. J., Nikolskaia, O., Kim, Y. V., Lonsdale-Eccles, J. D., Ito, S., Hara, T., … Kim, K. S. (2004). African trypanosome interactions with an in vitro model of the human blood-brain barrier. *Journal of Parasitology*, *90*(5), 970–979. https://doi.org/10.1645/GE-287R

Harker, K. S., Ueno, N., & Lodoen, M. B. (2015). *Toxoplasma gondii* dissemination: A parasite's journey through the infected host. *Parasite Immunology*, *37*(3), 141–149. https://doi.org/10.1111/pim.12163

Hirschhaeuser, F., Menne, H., Dittfeld, C., West, J., Mueller-Klieser, W., & Kunz-Schughart, L. A. (2010). Multicellular tumor spheroids: An underestimated tool is catching up again. *Journal of Biotechnology*, *148*, 3–15. https://doi.org/10.1016/j.jbiotec.2010.01.012

Howe, D. K., & Sibley, L. D. (1995). *Toxoplasma gondii* comprises three clonal lineages: Correlation of parasite genotype with human disease. *Journal of Infectious Diseases*, *172*(6), 1561–1566. https://doi.org/10.1093/infdis/172.6.1561

Huynh, M.-H., & Carruthers, V. B. (2006). Toxoplasma MIC2 is a major determinant of invasion and virulence. *PLoS Pathogens*, *2*(8), e84. https://doi.org/10.1371/journal.ppat.0020084

Juiz, N. A., Solana, M. E., Acevedo, G. R., Benatar, A. F., Ramirez, J. C., da Costa, P. A., … Schijman, A. G. (2017). Different genotypes of *Trypanosoma cruzi* produce distinctive placental environment genetic response in chronic experimental infection. *PLoS Neglected Tropical Diseases*, *11*(3), e0005436. https://doi.org/10.1371/journal.pntd.0005436

Juiz, N. A., Torrejón, I., Burgos, M., Torres, A. M. F., Duffy, T., Cayo, N. M., & Schijman, A. G. (2018). Alterations in placental gene expression of pregnant women with chronic Chagas disease. *The American Journal of Pathology*, *188*(6), 1345–1353. https://doi.org/10.1016/j.ajpath.2018.02.011

Kumar, H., & Tolia, N. H. (2019). Getting in: The structural biology of malaria invasion. *PLoS Pathogens*, *15*(9), e1007943. https://doi.org/10.1371/journal.ppat.1007943

Lambert, H., & Barragan, A. (2010). Modelling parasite dissemination: Host cell subversion and immune evasion by *Toxoplasma gondii*. *Cellular Microbiology*, *12*(3), 292–300. https://doi.org/10.1111/j.1462-5822.2009.01417.x

Lewis, M. D., Fortes Francisco, A., Taylor, M. C., Burrell-Saward, H., McLatchie, A. P., Miles, M. A., & Kelly, J. M. (2014). Bioluminescence imaging of chronic *Trypanosoma cruzi* infections reveals tissue-specific parasite dynamics and heart disease in the absence of locally persistent infection. *Cellular Microbiology*, *16*(9), 1285–1300. https://doi.org/10.1111/cmi.12297

Lewis, M. D., Francisco, A. F., Taylor, M. C., Jayawardhana, S., & Kelly, J. M. (2016). Host and parasite genetics shape a link between *Trypanosoma cruzi* infection dynamics and chronic cardiomyopathy. *Cellular Microbiology*, *18*(10), 1429–1443. https://doi.org/10.1111/cmi.12584

Lewis, M. D., Francisco, A. F., Taylor, M. C., & Kelly, J. M. (2015). A new experimental model for assessing drug efficacy against *Trypanosoma cruzi* infection based on highly sensitive *in vivo* imaging. *Journal of Biomolecular Screening*, *20*(1), 36–43. https://doi.org/10.1177/1087057114552623

Marinho, C. R. F., Nuñez-Apaza, L. N., Martins-Santos, R., Bastos, K. R. B., Bombeiro, A. L., Bucci, D. Z., & Álvarez, J. M. (2007). IFN-gamma, but not nitric oxide or specific IgG, is essential for the *in vivo* control of low-virulence Sylvio X10/4 *Trypanosoma cruzi* parasites. *Scandinavian Journal of Immunology*, *66*(2–3), 297–308. https://doi.org/10.1111/j.1365-3083.2007.01958.x

Marinho, C. R. F., Nuñez-Apaza, L. N., Bortoluci, K. R., Bombeiro, A. L., Bucci, D. Z., Grisotto, M. G., … Alvarez, J. M. (2009). Infection by the Sylvio X10/4 clone of *Trypanosoma cruzi*: Relevance of a low-virulence model of Chagas' disease. *Microbes and Infection*, *11*(13), 1037–1045. https://doi.org/10.1016/j.micinf.2009.07.011

Miller, S. A., Dykes, D. D., & Polesky, H. F. (1988). A simple salting out procedure for extracting DNA from human nucleated cells. *Nucleic Acids Research*, *16*(3), 1215. https://doi.org/10.1093/nar/16.3.1215

Mulenga, C., Mhlanga, J. D., Kristensson, K., & Robertson, B. (2001). *Trypanosoma brucei* brucei crosses the blood-brain barrier while tight junction proteins are preserved in a rat chronic disease model. *Neuropathology and Applied Neurobiology*, *27*(1), 77–85. https://doi.org/10.1046/j.0305-1846.2001.00306.x

Nikolskaia, O. V., Lima, A. P., Kim, Y. V., Lonsdale-Eccles, J. D., Fukuma, T., Scharfstein, J., & Grab, D. J. (2006). Blood-brain barrier traversal by African trypanosomes requires calcium signaling induced by parasite cysteine protease. *Journal of Clinical Investigation*, *116*(10), 2739–2747. https://doi.org/10.1172/JCI27798

OPS OMS. (2015). Enfermedad de Chagas. https://www.paho.org/es/temas/enfermedad-chagas

Postan, M., Dvorak, J. A., & McDaniel, J. P. (1983). Studies of *Trypanosoma cruzi* clones in inbred mice. I. A comparison of the course of infection

of C3H/HEN-mice with two clones isolated from a common source. *The American Journal of Tropical Medicine and Hygiene*, *32*(3), 497–506.

Prado, C. M., Jelicks, L. A., Weiss, L. M., Factor, S. M., Tanowitz, H. B., & Rossi, M. A. (2011). The vasculature in chagas disease. *Advances in Parasitology*, *76*, 83–99. https://doi.org/10.1016/B978-0-12-385895-5.00004-9

Ramakers, C., Ruijter, J. M., Deprez, R. H. L., & Moorman, A. F. (2003). Assumption-free analysis of quantitative real-time polymerase chain reaction (PCR) data. *Neuroscience Letters*, *339*(1), 62–66.

Rassi, A., Rassi, A., & Marin-Neto, J. A. (2010). Chagas disease. *The Lancet*, *375*(9723), 1388–1402.

Rodrigues, J. P. F., Souza Onofre, T., Barbosa, B. C., Ferreira, E. R., Bonfim-Melo, A., & Yoshida, N. (2019). Host cell protein LAMP-2 is the receptor for *Trypanosoma cruzi* surface molecule gp82 that mediates invasion. *Cellular Microbiology*, *21*(5), e13003. https://doi.org/10.1111/cmi.13003

Rodríguez, M. E., Rizzi, M., Caeiro, L., Masip, Y., Sánchez, D. O., & Tekiel, V. (2019). Transmigration of *Trypanosoma cruzi* Trypomastigotes through 3D spheroids mimicking host tissues. In *Methods in Molecular Biology* (Vol. 1955, pp. 165–177). New York, NY: Springer Protocols, Humana Press.

Rohland, S., Wechselberger, A., Spitzweg, C., Huss, R., Nelson, P. J., & Harz, H. (2015). Quantification of in vitro mesenchymal stem cell invasion into tumor spheroids using selective plane illumination microscopy. *Journal of Biomedical Optics*, *20*(4), 040501. https://doi.org/10.1117/1.JBO.20.4.040501

Santi-Rocca, J., Gironès, N., & Fresno, M. (2019). Multi-parametric evaluation of *Trypanosoma cruzi* infection. Outcome in animal models. In Methods in Molecular Biology. (Vol. 1955, pp.187–202). Clifton, NJ: Springer Protocols, Humana Press. https://doi.org/10.1007/978-1-4939-9148-8_14

Schenkman, S., & Mortara, R. A. (1992). HeLa cells extend and internalize pseudopodia during active invasion by *Trypanosoma cruzi* trypomastigotes. *Journal of Cell Science*, *101*, 895–905.

Schneider, C. A., Rasband, W. S., & Eliceiri, K. W. (2012). NIH image to ImageJ: 25 years of image analysis. *Nature Methods*, *9*(7), 671–675. https://doi.org/10.1038/nmeth.2089

Shamir, E. R., & Ewald, A. J. (2014). Three-dimensional organotypic culture: Experimental models of mammalian biology and disease. *Nature Reviews Molecular Cell Biology*, *15*(10), 647–664. https://doi.org/10.1038/nrm3873

Stuelten, C. H., Parent, C. A., & Montell, D. J. (2018). Cell motility in cancer invasion and metastasis: Insights from simple model organisms. *Nature Reviews Cancer*, *18*(5), 296–312. https://doi.org/10.1038/nrc.2018.15

Volta, B. J., Bustos, P. L., Cardoni, R. L., De Rissio, A. M., Laucella, S. A., & Bua, J. (2016). Serum cytokines as biomarkers of early *Trypanosoma cruzi* infection by congenital exposure. *The Journal of Immunology*, *196*(11), 4596–4602. https://doi.org/10.4049/jimmunol.1502504

Weight, C. M., Jones, E. J., Horn, N., Wellner, N., & Carding, S. R. (2015). Elucidating pathways of toxoplasma gondii invasion in the gastrointestinal tract: Involvement of the tight junction protein occludin. *Microbes and Infection*, *17*(10), 698–709. https://doi.org/10.1016/j.micinf.2015.07.001

Wolf, K., & Friedl, P. (2011). Extracellular matrix determinants of proteolytic and non-proteolytic cell migration. *Trends in Cell Biology*, *21*(12), 736–744. https://doi.org/10.1016/j.tcb.2011.09.006

Yang, A. S. P., O'Neill, M. T., Jennison, C., Lopaticki, S., Allison, C. C., Armistead, J. S., & Boddey, J. A. (2017). Cell traversal activity is important for *Plasmodium falciparum* liver infection in humanized mice. *Cell Reports*, *18*(13), 3105–3116. https://doi.org/10.1016/j.celrep.2017.03.017

Zanoni, M., Piccinini, F., Arienti, C., Zamagni, A., Santi, S., Polico, R., … Tesei, A. (2016). 3D tumor spheroid models for in vitro therapeutic screening: A systematic approach to enhance the biological relevance of data obtained. *Scientific Reports*, *6*(1), 19103. https://doi.org/10.1038/srep19103

Zingales, B., Miles, M. A., Campbell, D. A., Tibayrenc, M., Macedo, A. M., Teixeira, M. M. G., & Sturm, N. R. (2012). The revised *Trypanosoma cruzi* subspecific nomenclature: Rationale, epidemiological relevance and research applications. *Infection, Genetics and Evolution*, *12*(2), 240–253. https://doi.org/10.1016/j.meegid.2011.12.009

SUPPORTING INFORMATION

Additional supporting information may be found online in the Supporting Information section at the end of this article.

How to cite this article: Rodríguez ME, Rizzi M, Caeiro LD, et al. Transmigration of *Trypanosoma cruzi* trypomastigotes through 3D cultures resembling a physiological environment. *Cellular Microbiology*. 2020;22:e13207. https://doi.org/10.1111/cmi.13207